Electronic Supplementary Material (ESI) for Journal of Materials Chemistry C.

Supporting information

Inverting Substitution Patterns on Amphiphilic Cyclodextrins Induces Unprecedented Formation of Hexagonal Columnar Superstructures

Pier-Luc Champagne,[a] David Ester,[b] Michael Zeeman[b], Carson Zellman,[b] Vance E. Williams,[b]* Chang-Chun Ling [a]*

[a]Alberta Glycomics Centre, Department of Chemistry, University of Calgary, Calgary, Alberta T2N 1N4 Canada

[b]Department of Chemistry, Simon Fraser University, Burnaby, BC V5A 1S6 Canada.

*Email: vancew@sfu.ca; ccling@ucalgary.ca

Table of Contents

A: NMR spectra of synthesized compounds

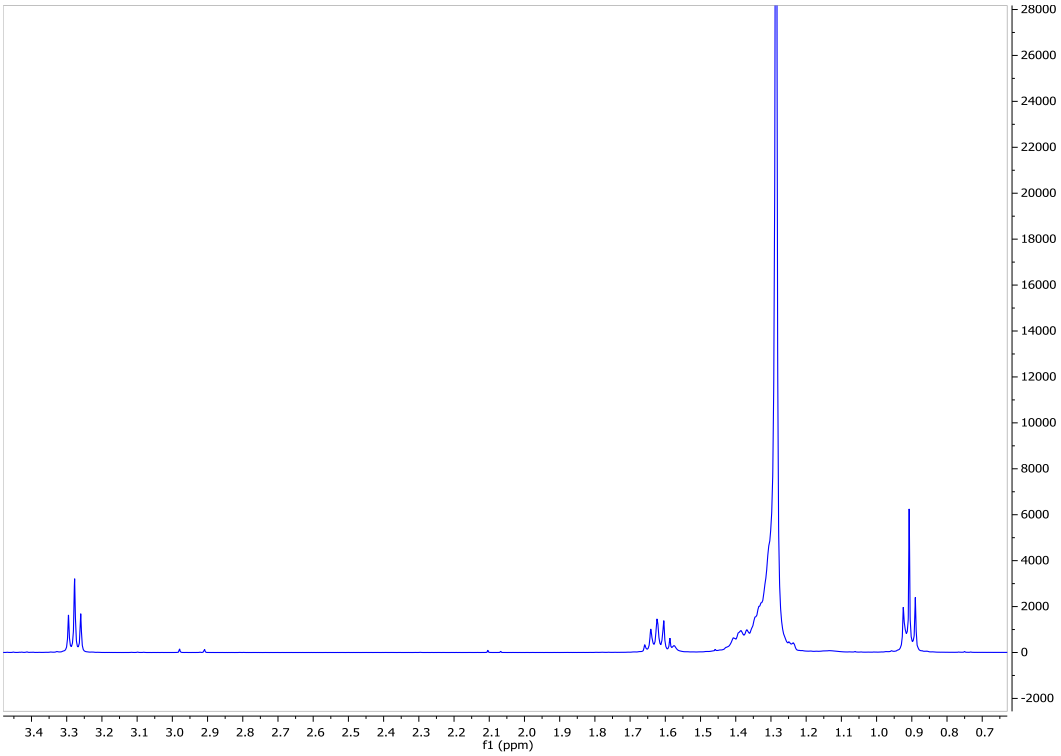

Figure S1. ^{1}H NMR spectra 400 MHz of 1-azidoctadecane **(8)** in $CDCl_3$

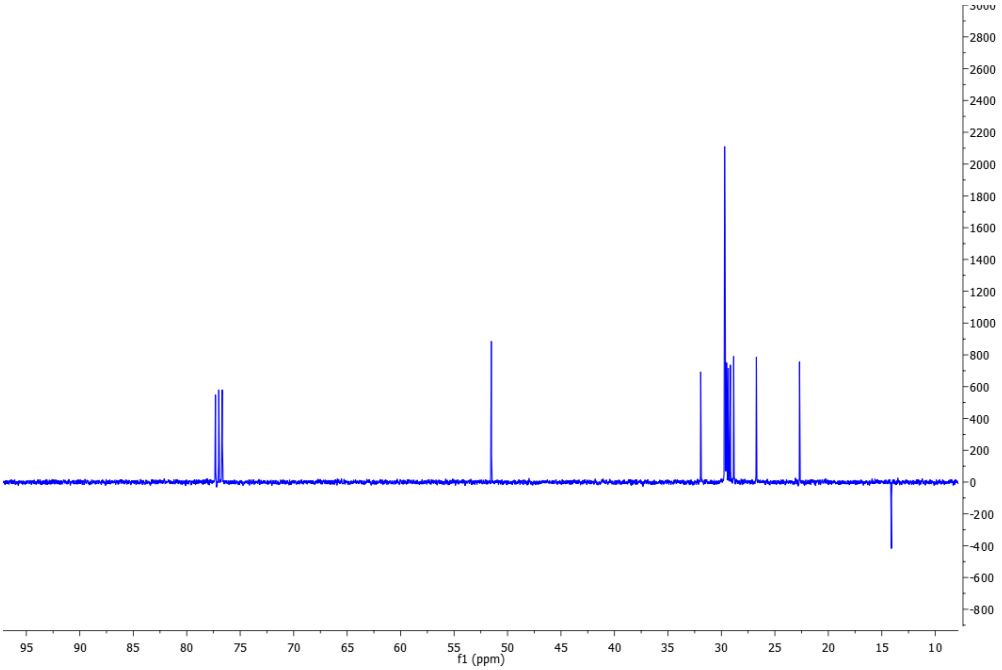

Figure S2. ^{13}C DEPT-Q NMR spectra 400 MHz of 1-azidoctadecane **(8)** in $CDCl_3$

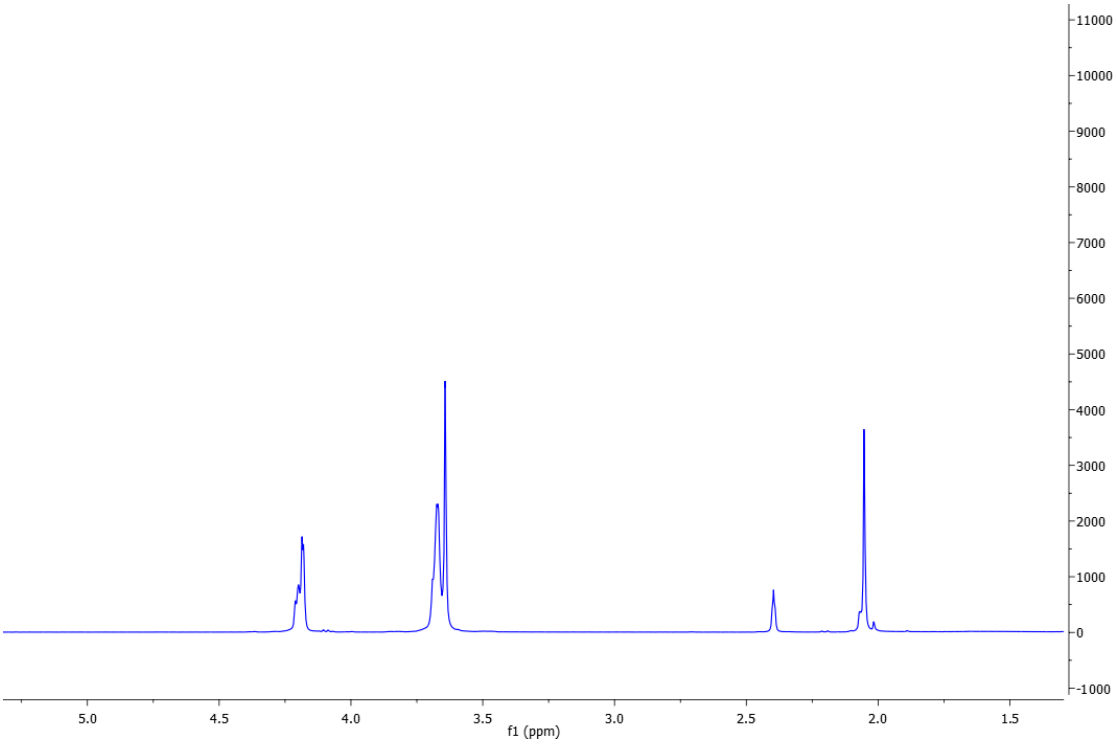

Figure S3. ^{1}H NMR spectra 400 MHz of 2-(2-propargylethoxy)ethyl acetate **(13)** in $CDCl_3$

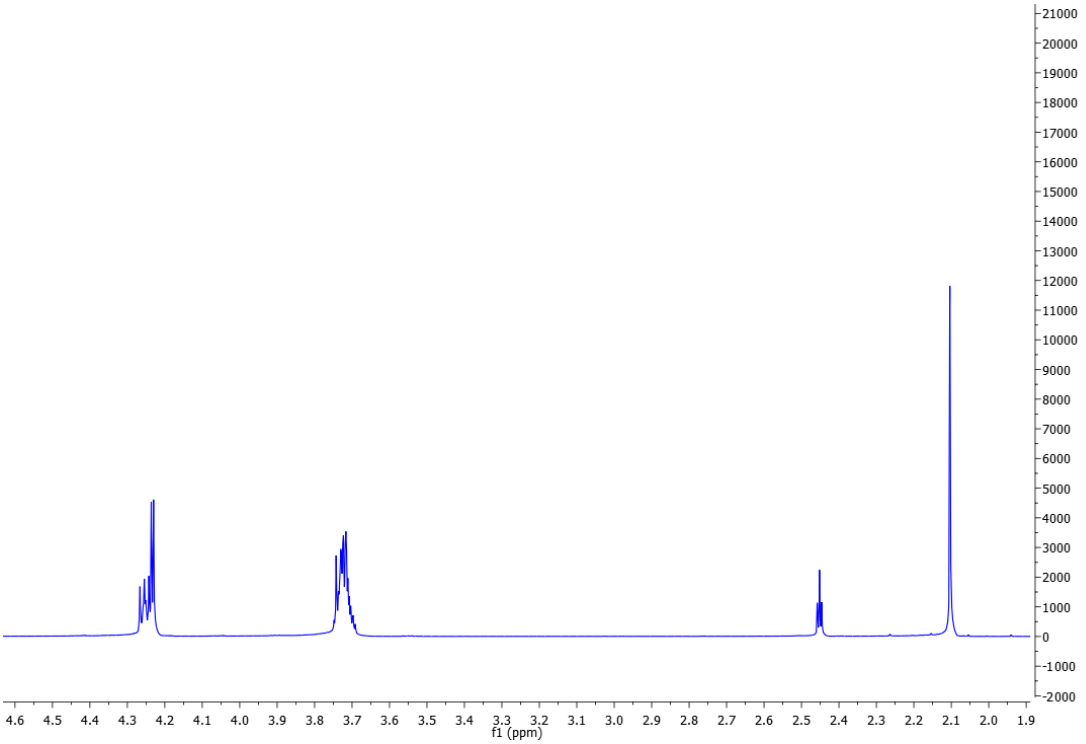

Figure S4. ^{1}H NMR spectra 400 MHz of (2-(2-(2-propargylethoxy)ethoxy)ethyl acetate **(14)** in $CDCl_3$

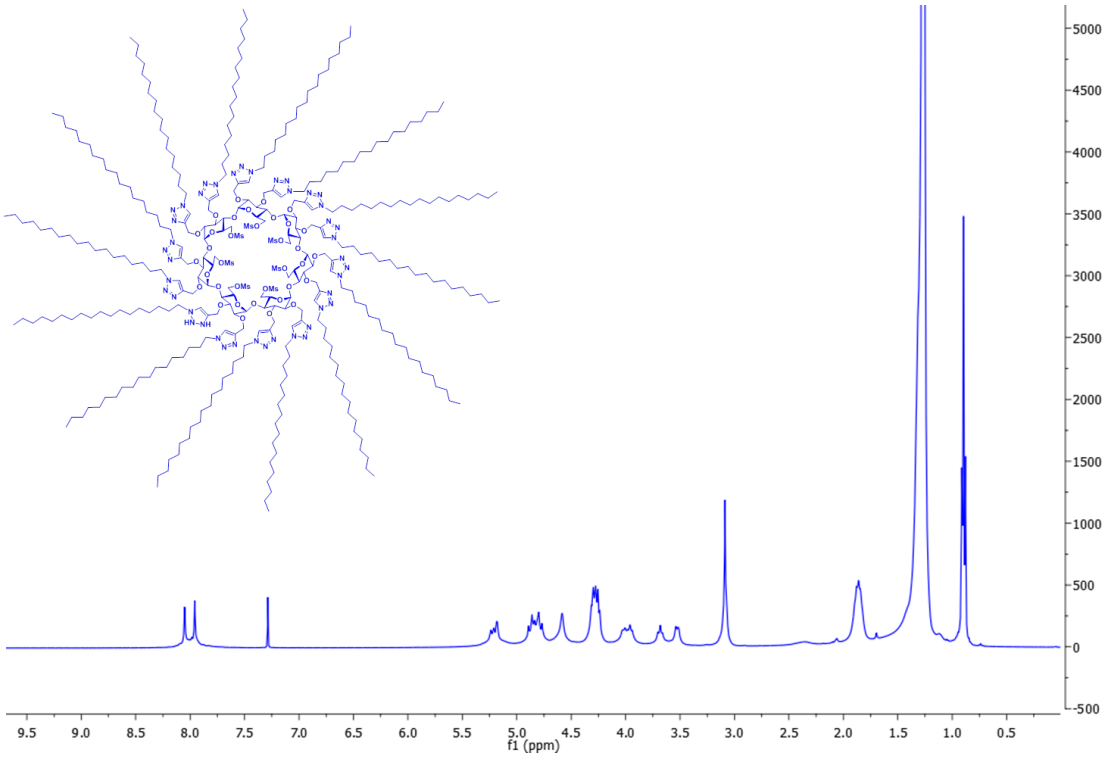

Figure S5. ^{1}H NMR spectra 400 MHz of per-2,3-di-O-(1-octadecyl-1*H*-1,2,3-triazol-4-yl)methyl-6-*O*-mesyl-β-cyclodextrin **(9)** in $CDCl_3$

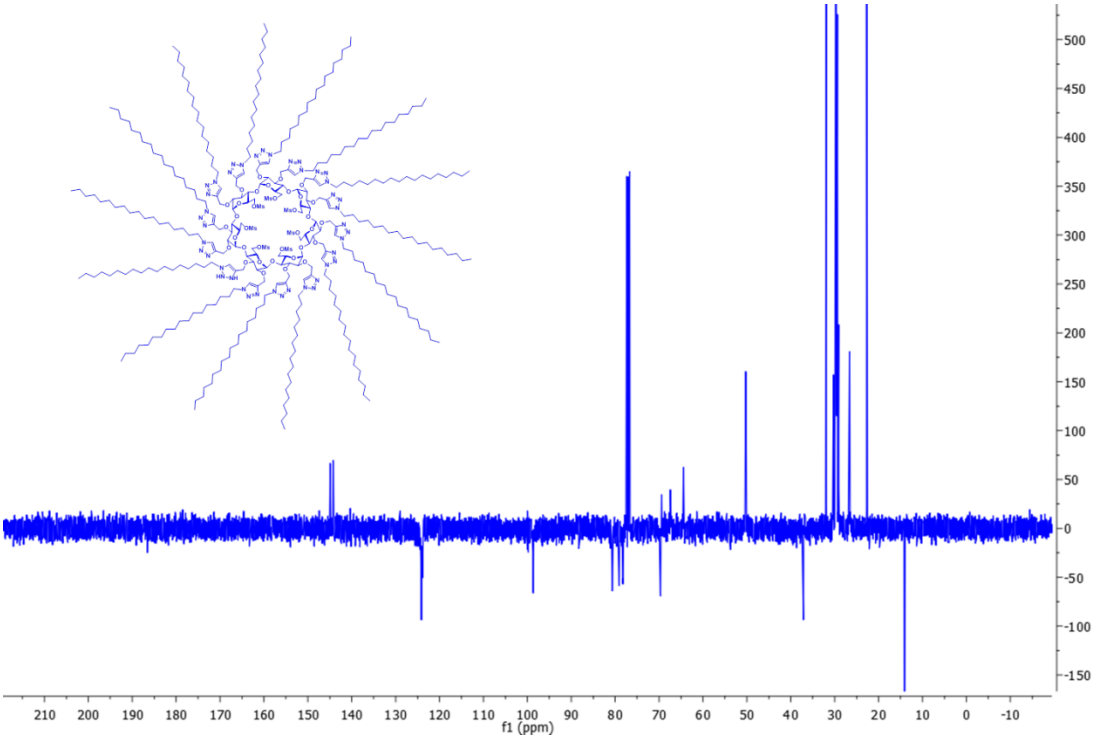

Figure S6. ^{13}C DEPT-Q NMR 101 MHz spectra of per-2,3-di-O-(1-octadecyl-1*H*-1,2,3-triazol-4-yl)methyl-6-*O*-mesyl-β-cyclodextrin **(9)** in $CDCl_3$

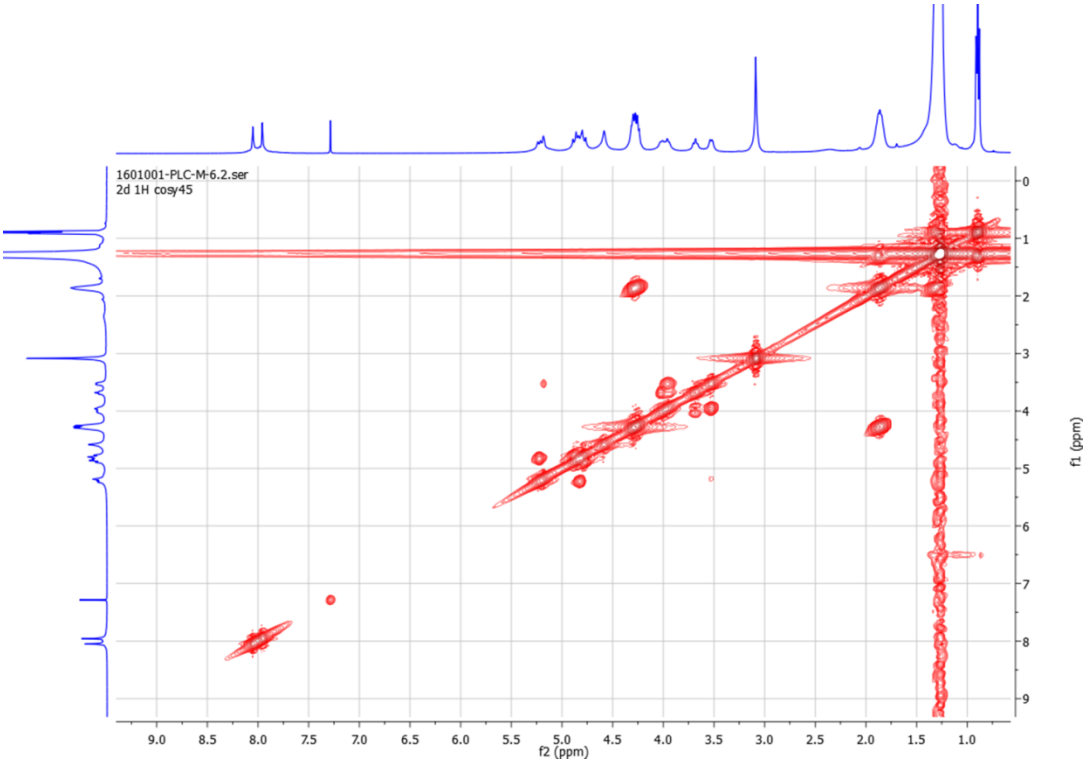

Figure S7. ^{1}H ^{1}H 2D COSY NMR spectra of per-2,3-di-O-(1-octadecyl-1*H*-1,2,3-triazol-4-yl)methyl-6-*O*-mesyl-β-cyclodextrin **(9)** 400 MHZ in $CDCl_3$

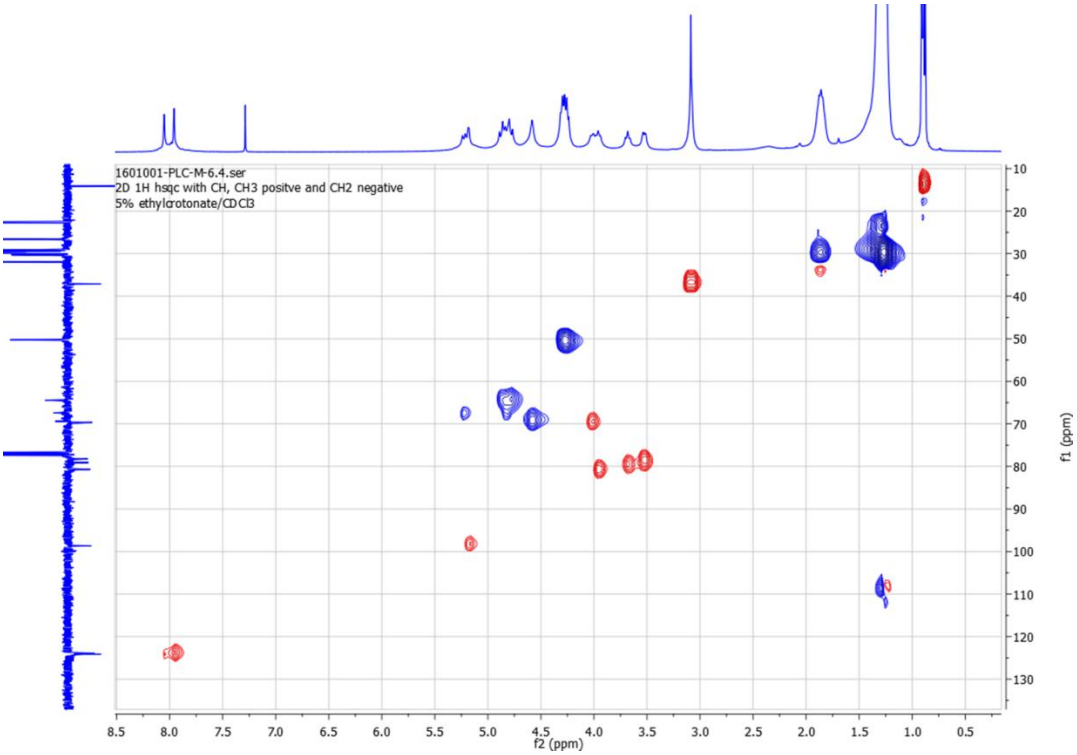

Figure S8. ^{1}H ^{13}C 2D HSQC 400 MHz NMR specta of per-2,3-di-O-(1-octadecyl-1*H*-1,2,3-triazol-4-yl)methyl-6-*O*-mesyl-β-cyclodextrin **(9)** 400 MHZ in $CDCl_3$

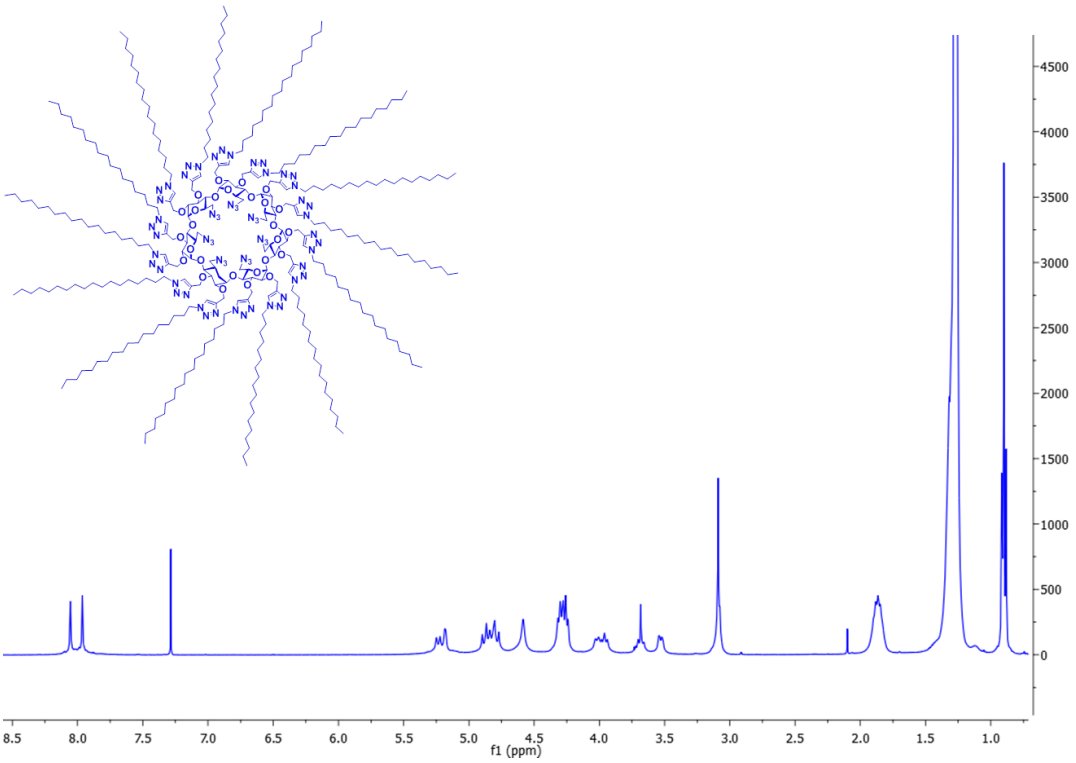

Figure S9. ^{1}H NMR spectra 400 MHz of per-6-azido-6-deoxy-2,3-di-*O*-(1-octadecyl-1*H*-1,2,3-triazol-4-yl)methyl-β-cyclodextrin **(10)** in $CDCl_3$

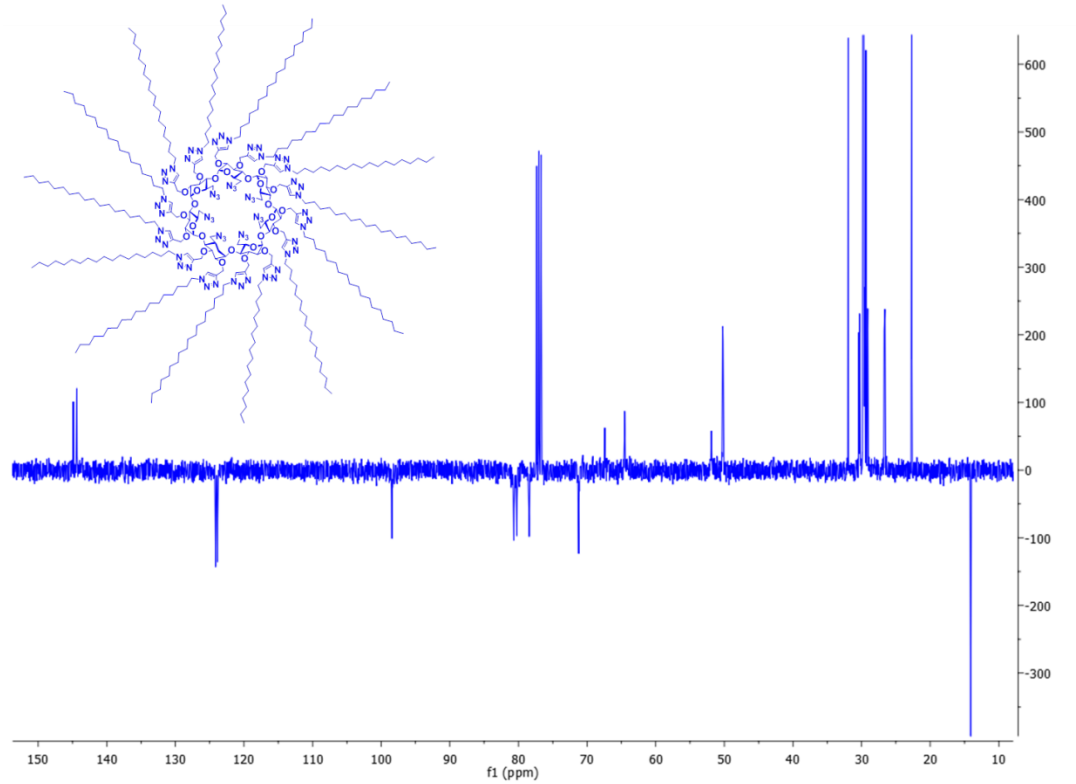

Figure S10. ^{13}C DEPT-Q NMR spectra 101 MHz of per-6-azido-6-deoxy-2,3-di-*O*-(1-octadecyl-1*H*-1,2,3-triazol-4-yl)methyl-β-cyclodextrin **(10)** in $CDCl_3$

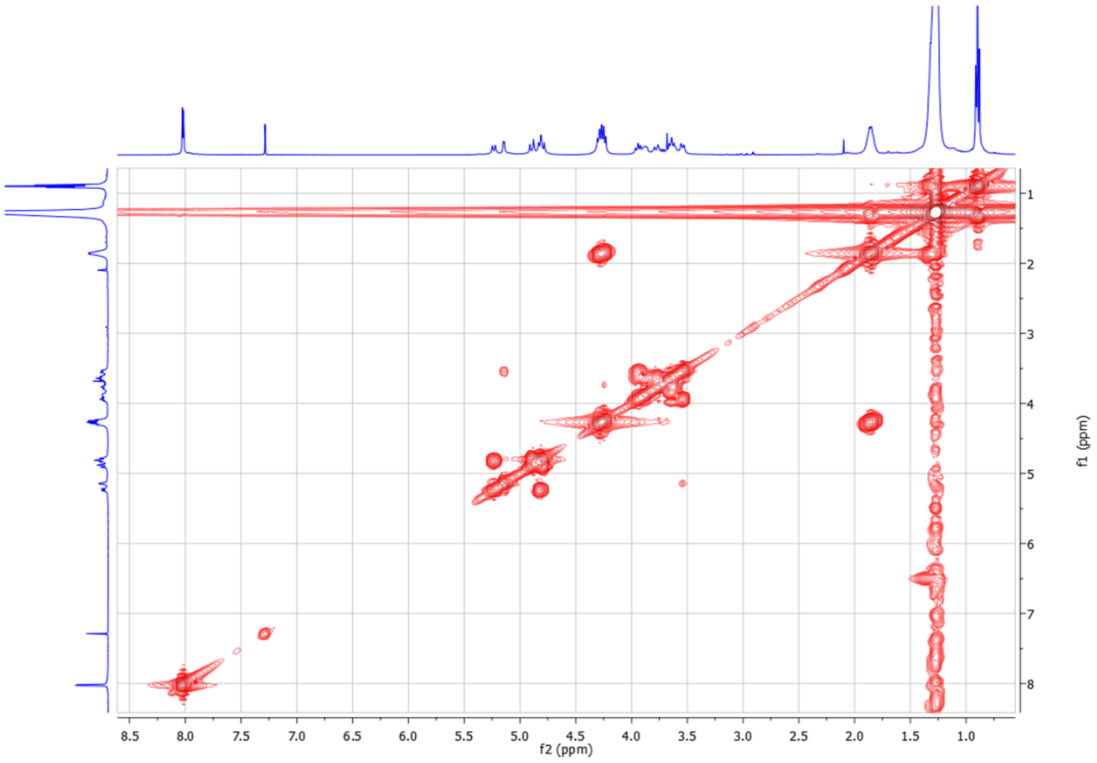

Figure S11. ^{1}H ^{1}H 2D COSY NMR spectra of per-6-azido-6-deoxy-2,3-di-*O*-(1-octadecyl-1*H*-1,2,3-triazol-4-yl)methyl-β-cyclodextrin **(10)** in $CDCl_3$

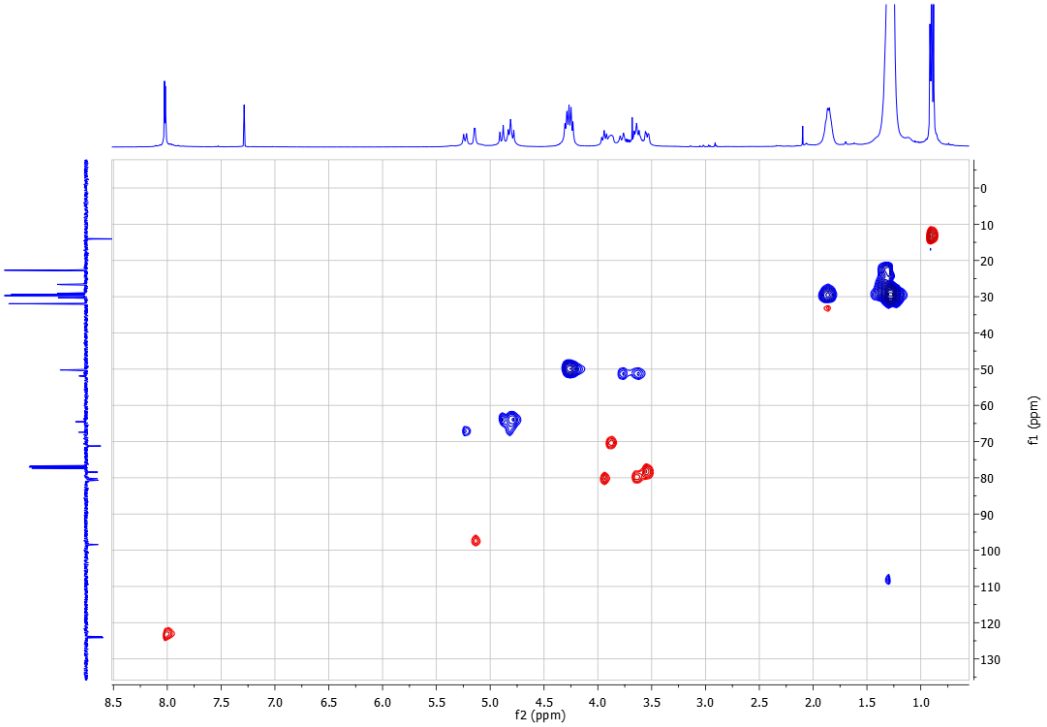

Figure S12. ^{1}H ^{13}C 2D HSQC 400 MHz NMR spectra of per-6-azido-6-deoxy-2,3-di-*O*-(1-octadecyl-1*H*-1,2,3-triazol-4-yl)methyl-β-cyclodextrin **(10)** in $CDCl_3$

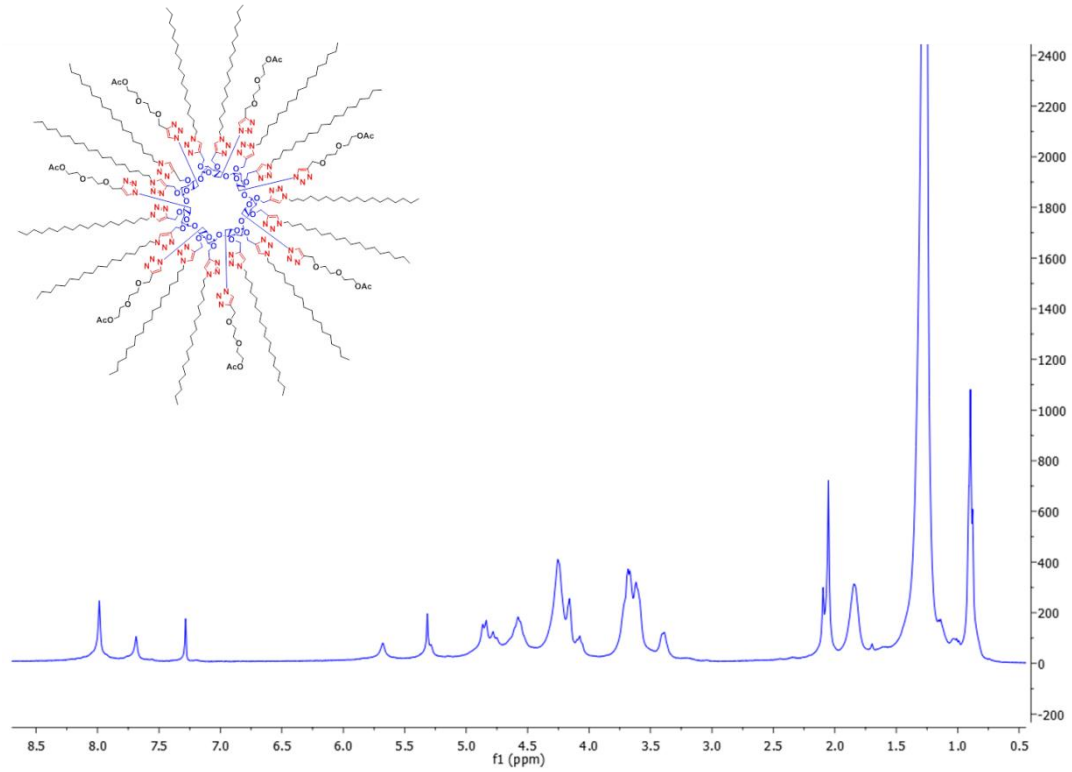

Figure S13. ^{1}H NMR spectra 400 MHz of compound **(4)** in $CDCl_3$

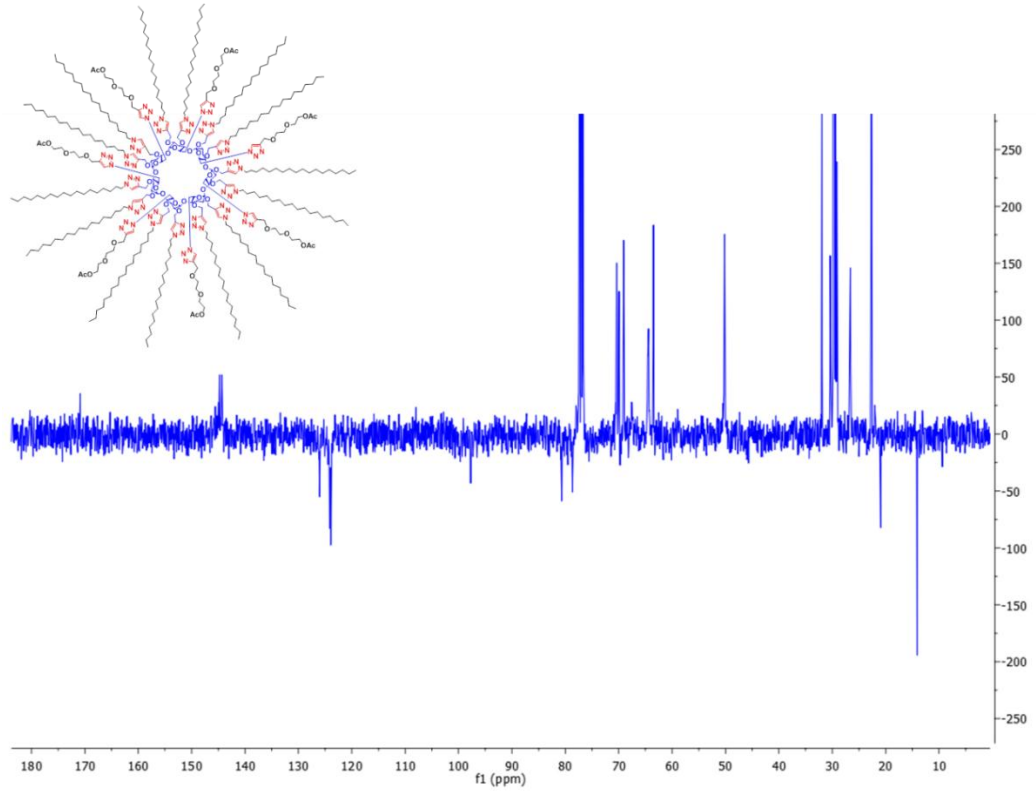

Figure S14. ^{13}C NMR DEPT-Q spectra 101 MHz of compound **(4)** in $CDCl_3$

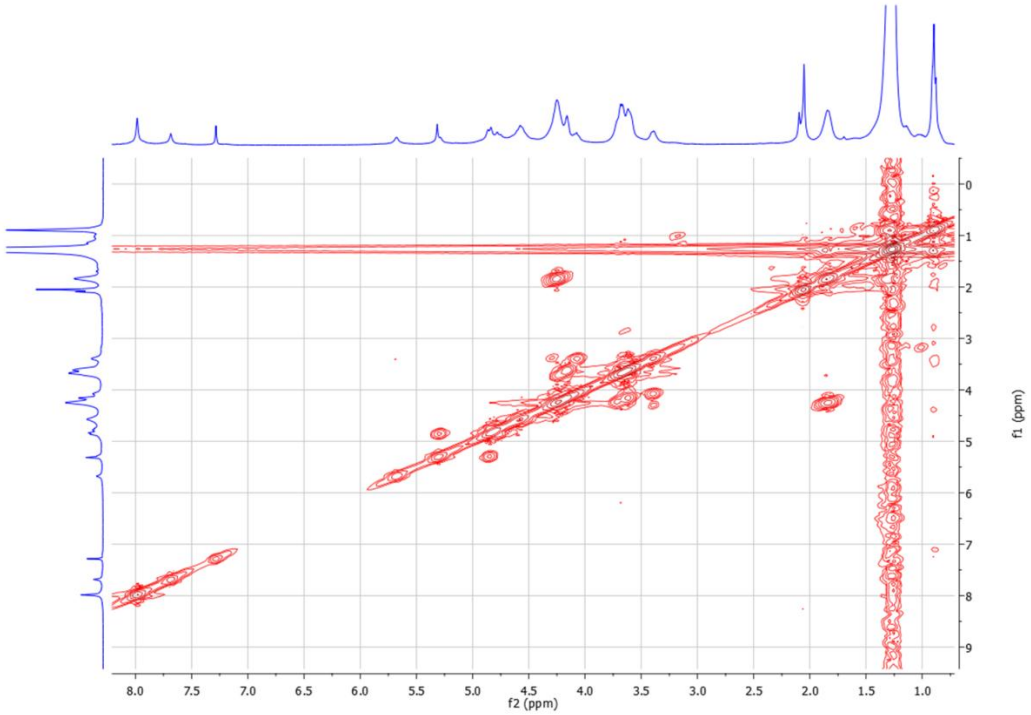

Figure S15. ^{1}H ^{1}H 2D COSY NMR spectra of compound **(4)** in $CDCl_3$

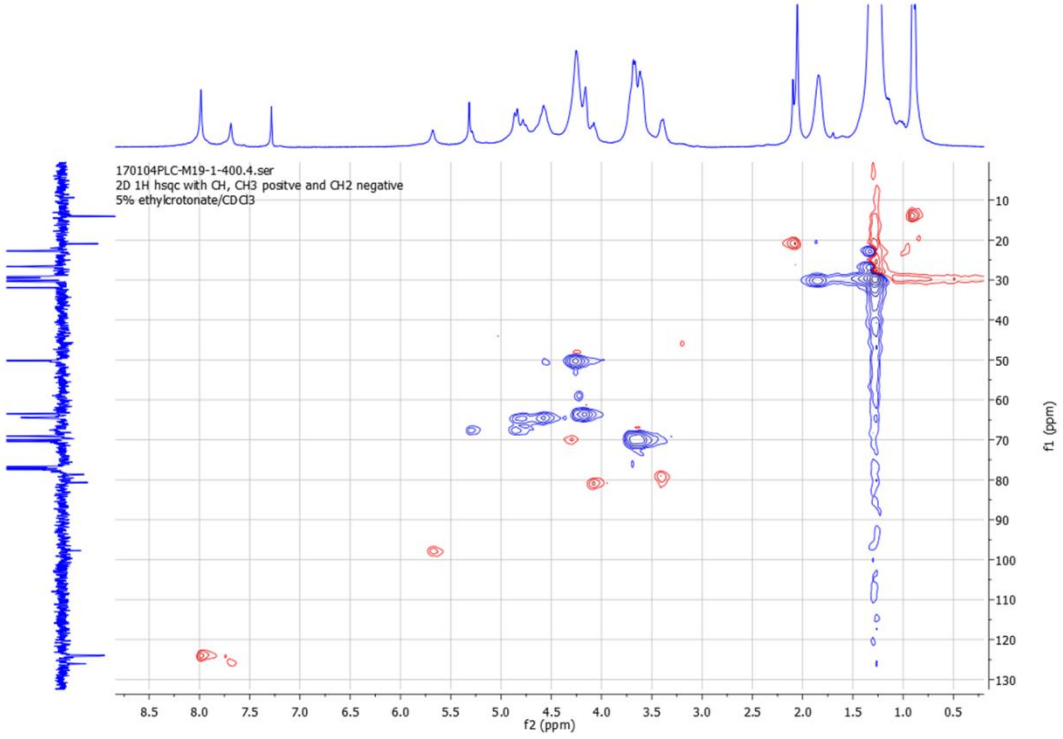

Figure S16. ^{1}H ^{13}C 2D HSQC 400 MHz NMR spectra of compound **(4)** in $CDCl_3$

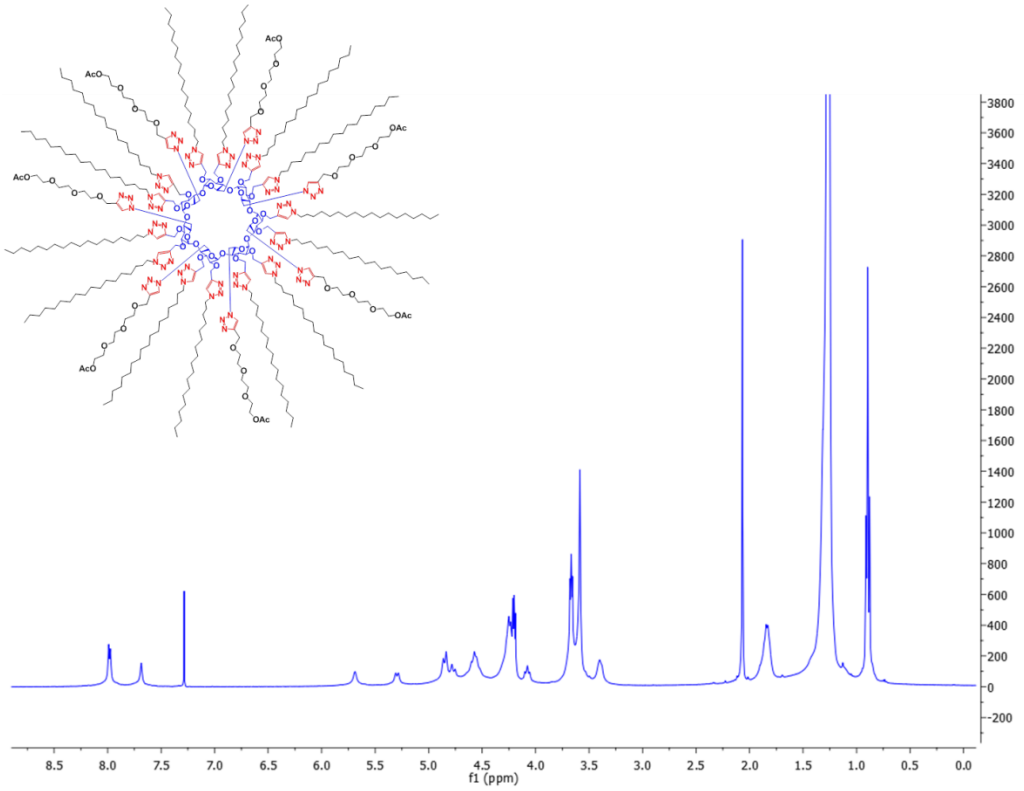

Figure S17. ^{1}H NMR spectra 400 MHz of compound **(5)** in $CDCl_3$

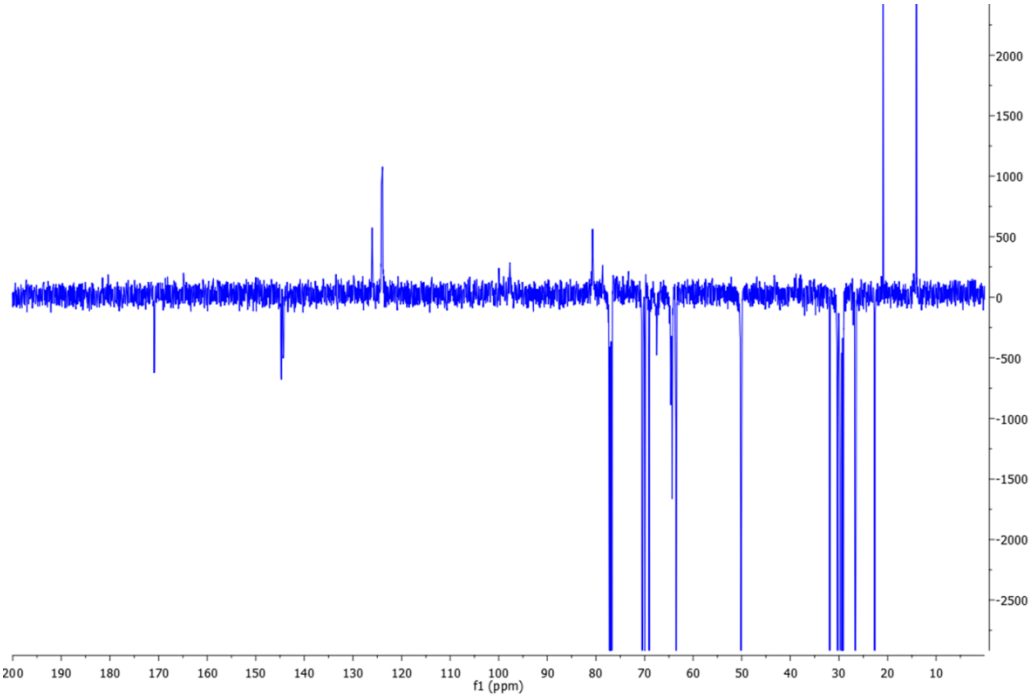

Figure S18. ^{13}C DEPT-Q NMR spectra 101 MHz of compound **(4)** in $CDCl_3$

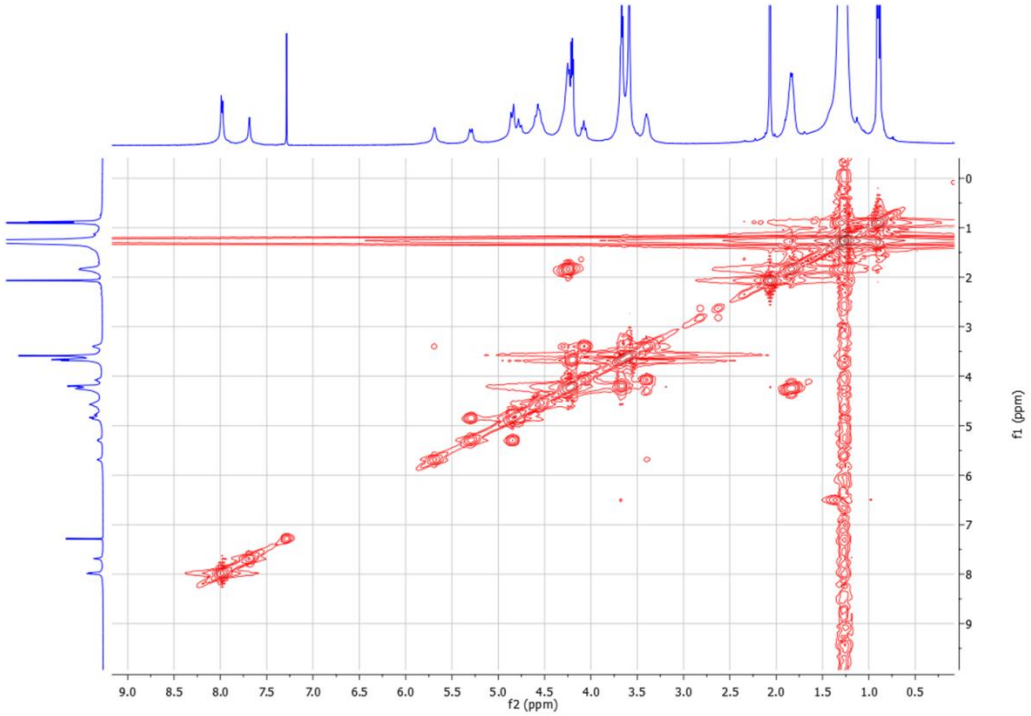

Figure S19. ^{1}H ^{1}H 2D COSY NMR spectra of compound **(5)** in $CDCl_3$

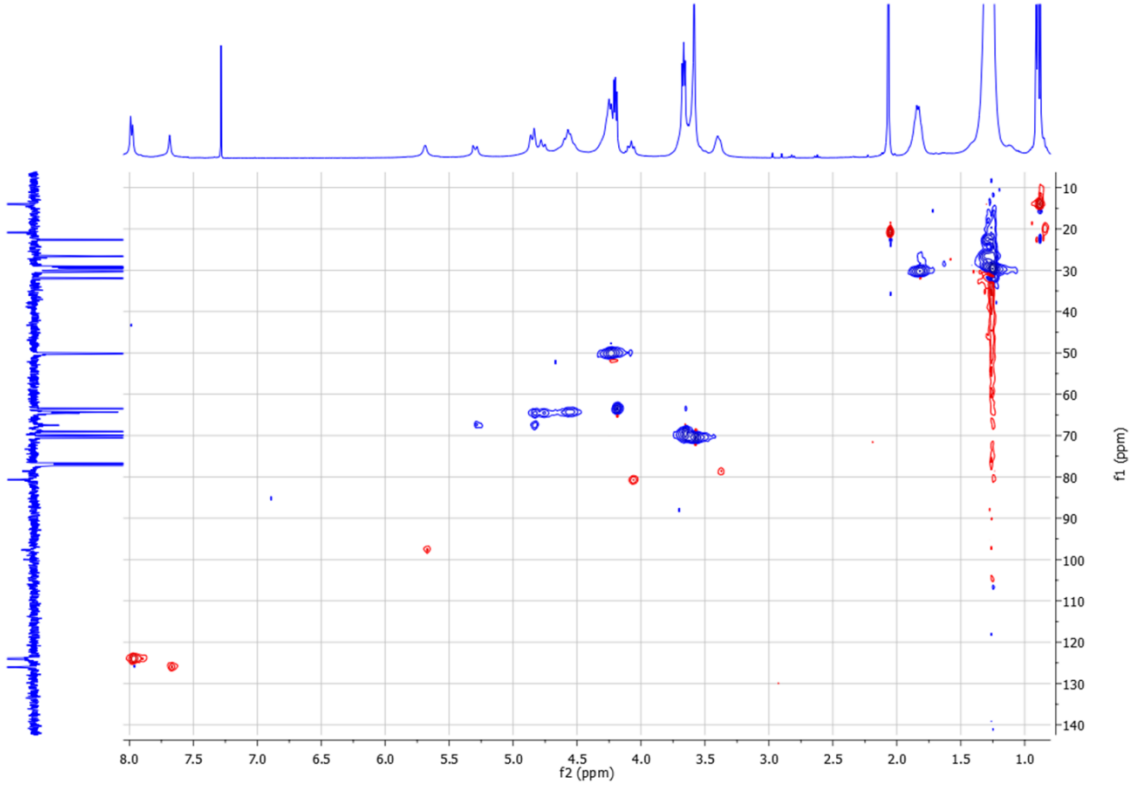

Figure S20. ^{1}H ^{13}C 2D HSQC 400 MHz NMR spectra of compound **(5)** in $CDCl_3$

B: Thermogravimetric Analysis

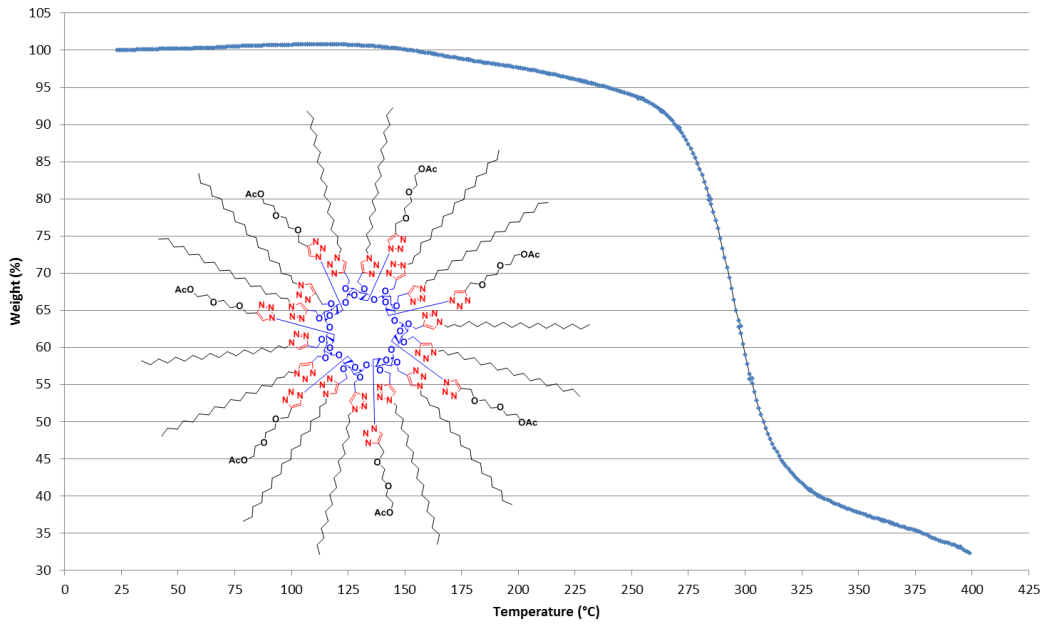

Figure S21. Thermogravimetric analysis of compound **4** (2˚C/min)

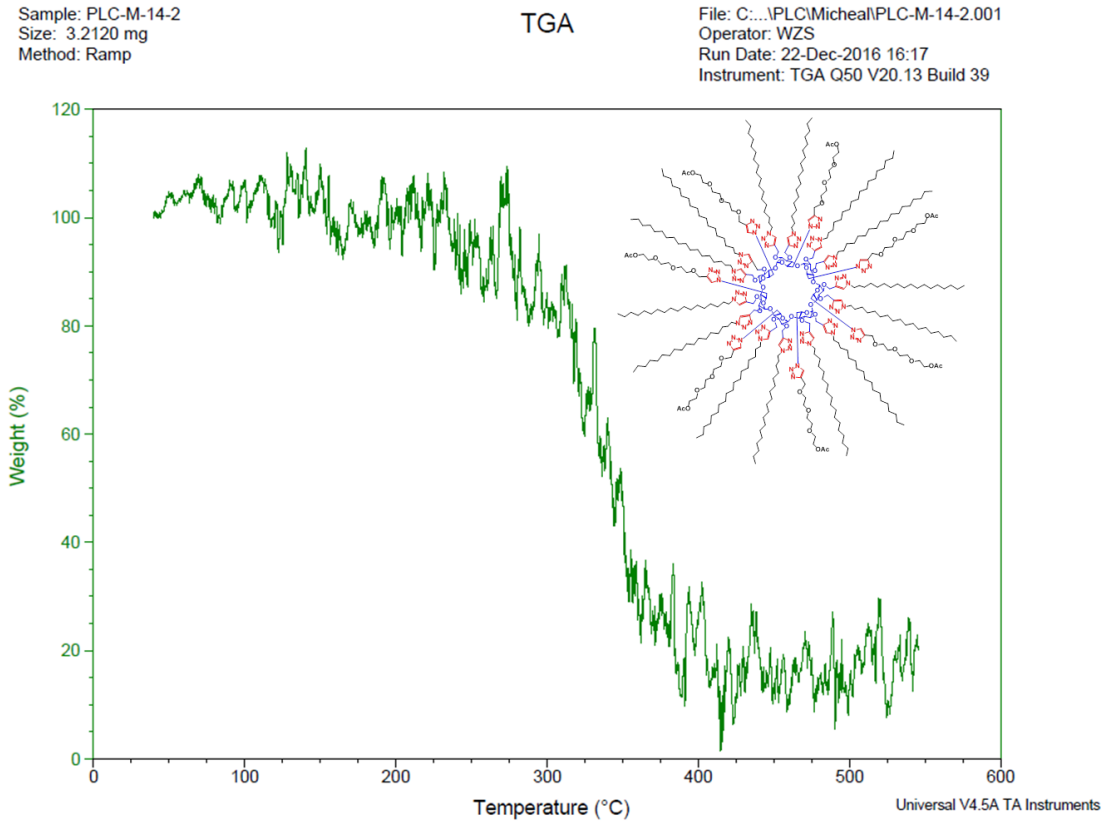

Figure S22. Thermogravimetric analysis of compound **5** (10˚C/min)

C: X-ray Diffraction Analysis

Table S1. XRD data for the compounds studied, including comparison of experimentally observed d-spacings and calculated values based on $\frac{1}{d^2} = \frac{4}{3}\frac{(h^2+hk+k^2)}{a^2} + \frac{l^2}{c^2}$. PLC-M-14 is compound **4**; PLC-M-19 is compound **5**.

Compound	Temperature (˚C)	Phase (a/Å)	d-spacing, observed (Å)	d-spacing, calculated (Å)	Miller indices
PLC-M-14	25	Col_h (66.6)	57.7	57.7	d_{100}
			32.3	33.3	d_{110}
			28.4	28.8	d_{200}
			20.9	21.8	d_{210}
			4.13		alkyl halo
	100	Col_h (61.7)	53.5	53.5	d_{100}
			30.5	30.9	d_{110}
			26.8	26.7	d_{200}
			20.2	20.2	d_{210}
			4.72		alkyl halo
	175	isotropic	48.7		--
			29.5		--
			4.79		alkyl halo
PLC-M-19	25	Col_h (62.5)	54.1	54.1	d_{100}
			30.7	31.3	d_{110}
			27.3	27.1	d_{200}
			20.0	20.5	d_{210}
			4.13		alkyl halo
	100	Col_h (58.9)	51.0	51.0	d_{100}
			29.3	29.4	d_{110}
			25.9	25.5	d_{200}
			19.3	19.3	d_{210}
			4.75		alkyl halo
	140	isotropic	48.2		--
			31.4		--
			4.76		alkyl halo

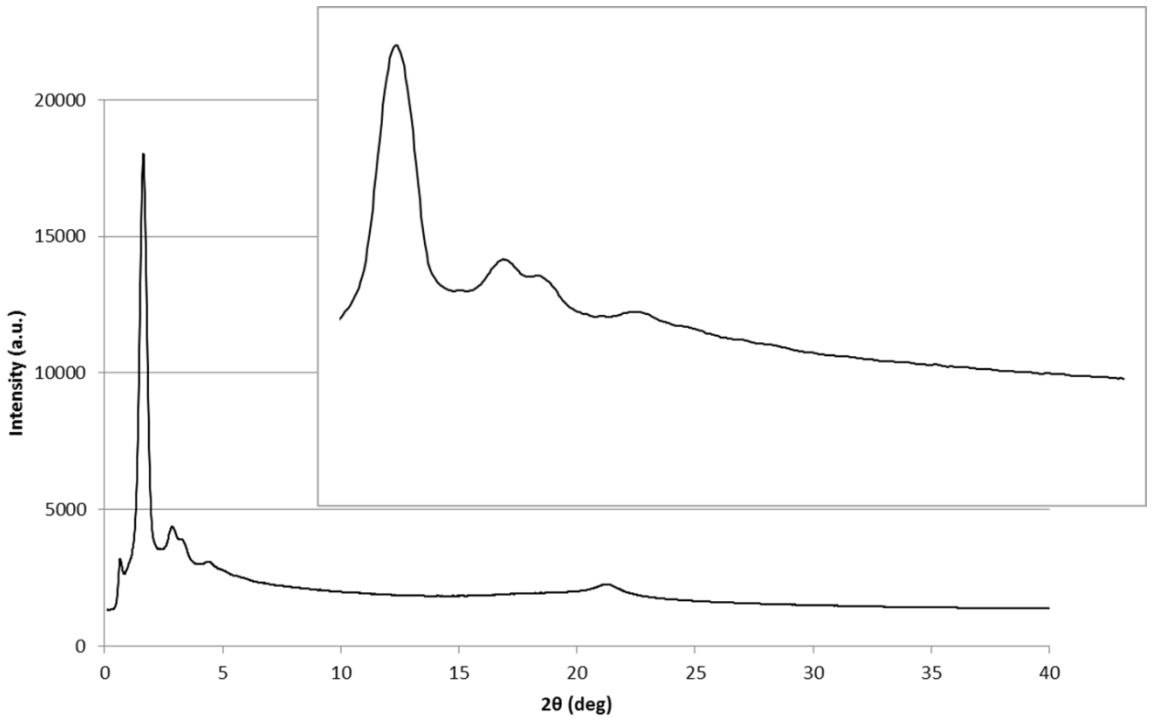

Figure S23. XRD spectra of **β-CD-4** at 25˚C

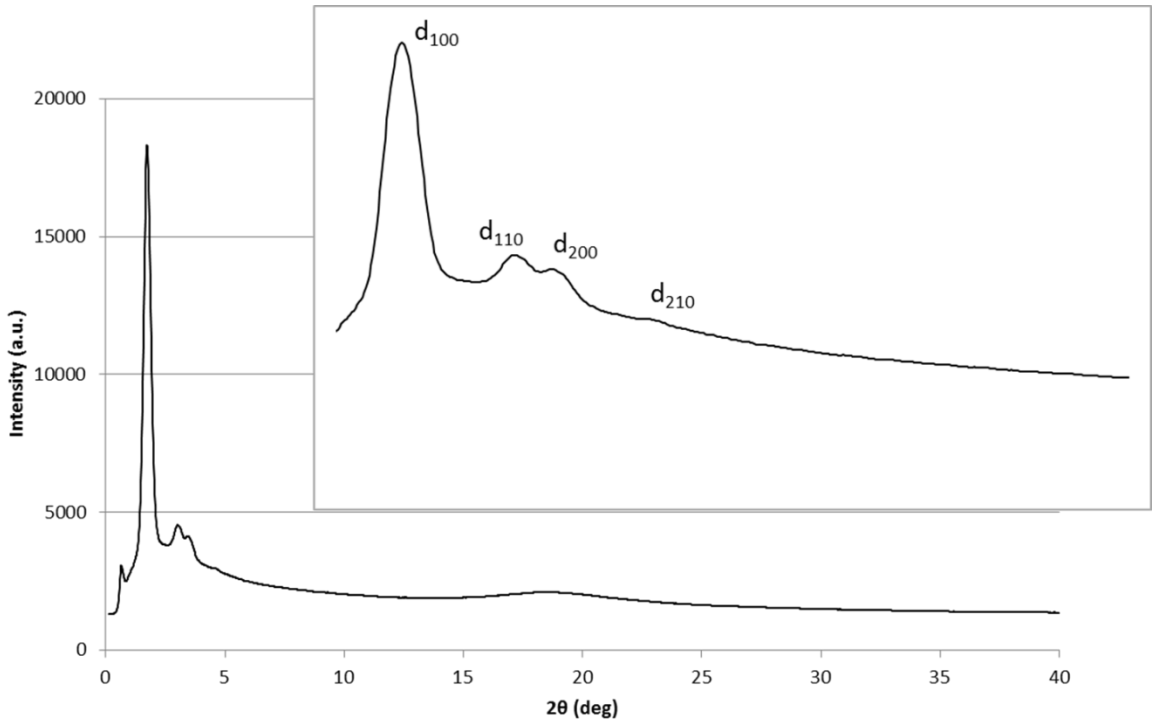

Figure S24. XRD spectra of **β-CD-4** at 100˚C

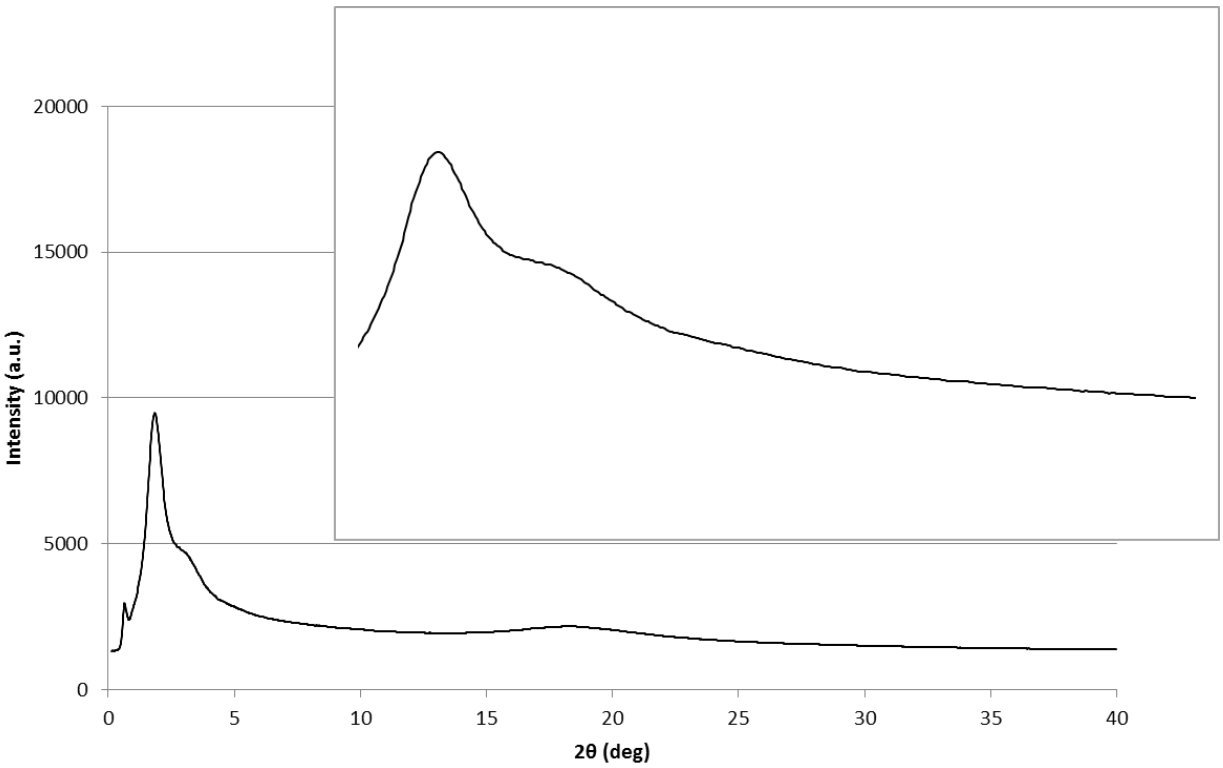

Figure S25. XRD spectra of **β-CD-4** at 140˚C

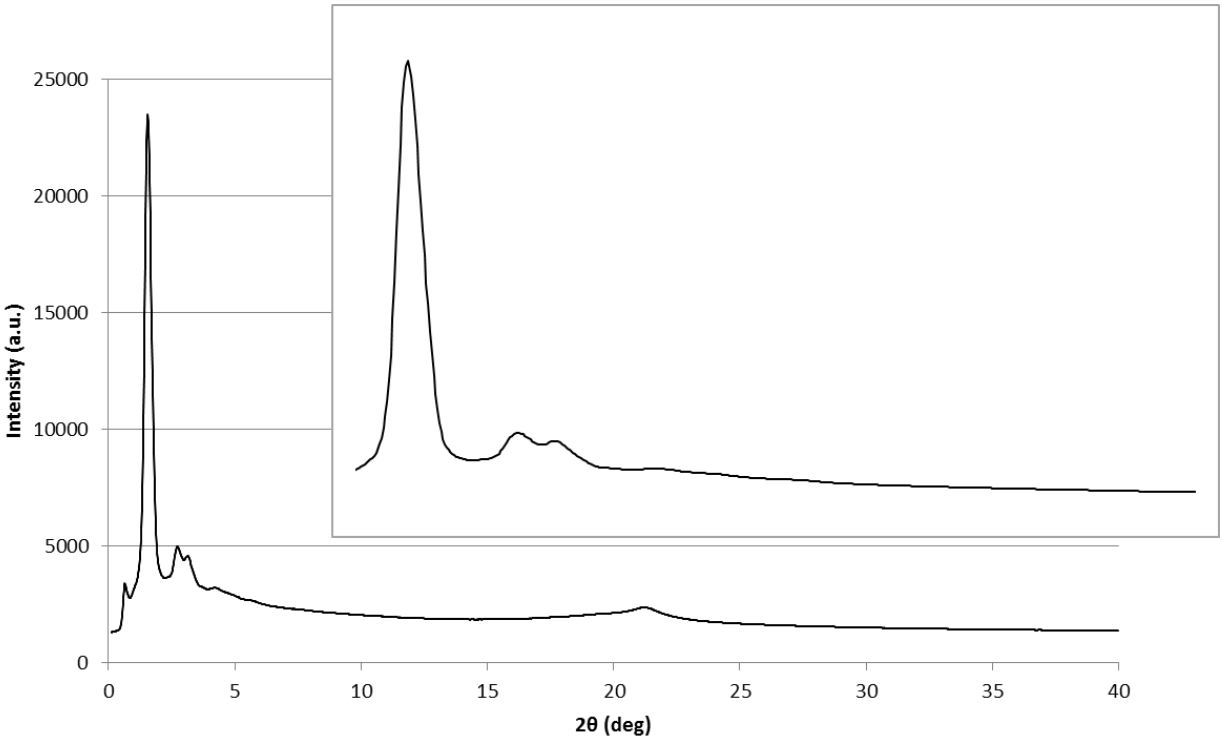

Figure S26. XRD spectra of **β-CD-5** at 25˚C

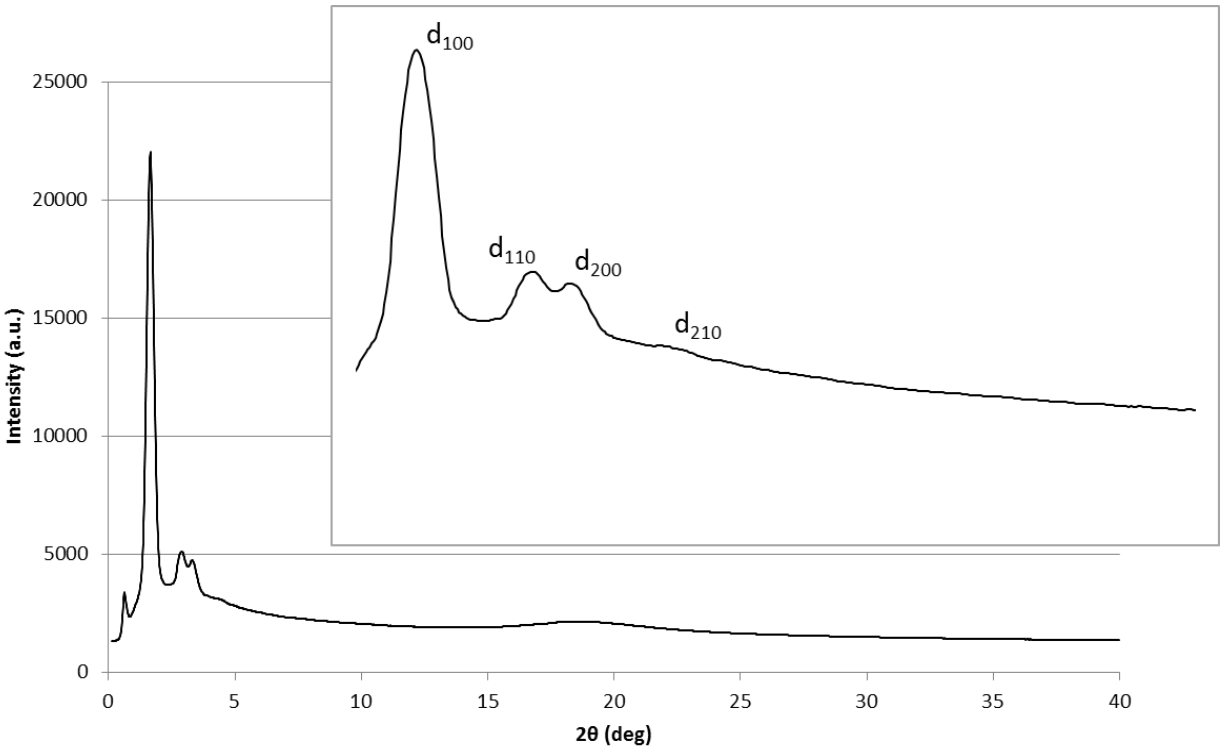

Figure S27. XRD spectra of **β-CD-5** at 100˚C

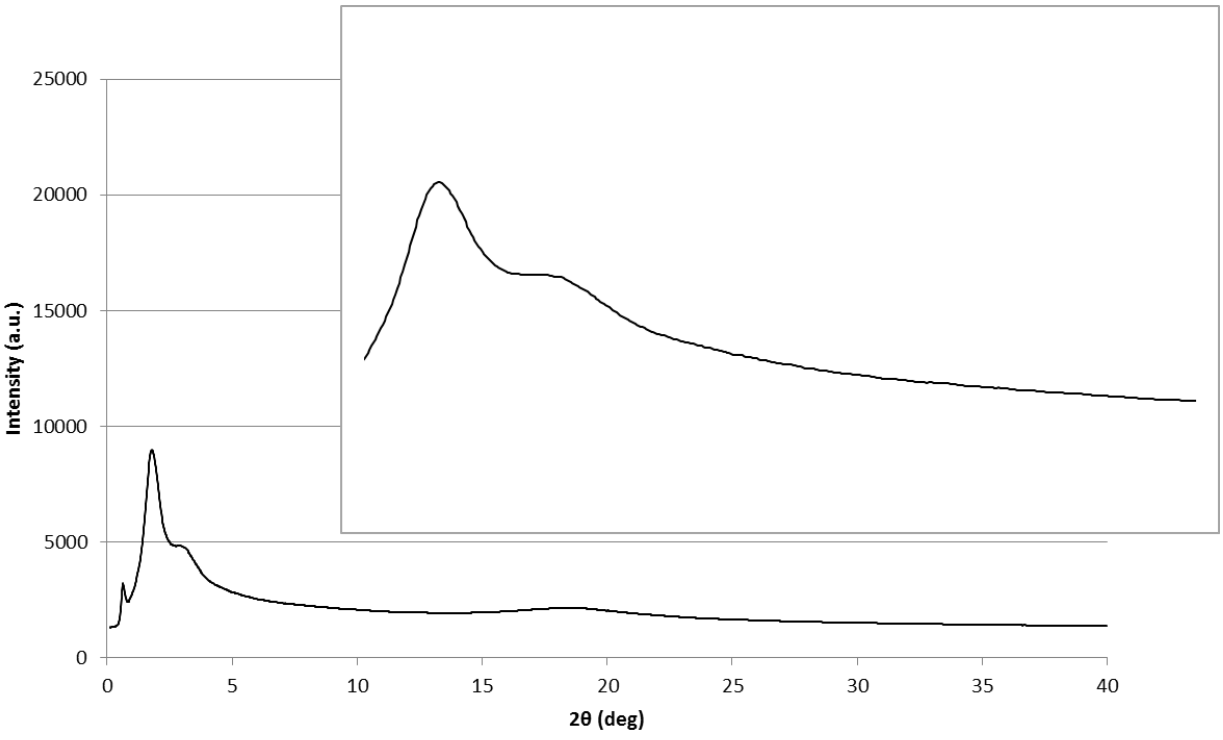

Figure S28. XRD spectra of **β-CD-5** at 275˚C

D: Differential Scanning Calorimetry Analysis

Table S2. Phase transitions of **β-CD-4** and **5** recorded by DSC

Compound	1st Phase Transition, heating/cooling	2nd Phase Transition, heating/cooling
PLC-M-14	51.0 ˚C (30.6 J/g)/ 38.1 ˚C (28.0 J/g)	141.9 ˚C (0.72 J/g)/ 138.9 ˚C (0.77 J/g)
PLC-M-19	48.4 ˚C (26.8 J/g)/ 36.1 ˚C (23.5 J/g)	126.8 ˚C (0.34 J/g)/ 123.9 ˚C (0.20 J/g)

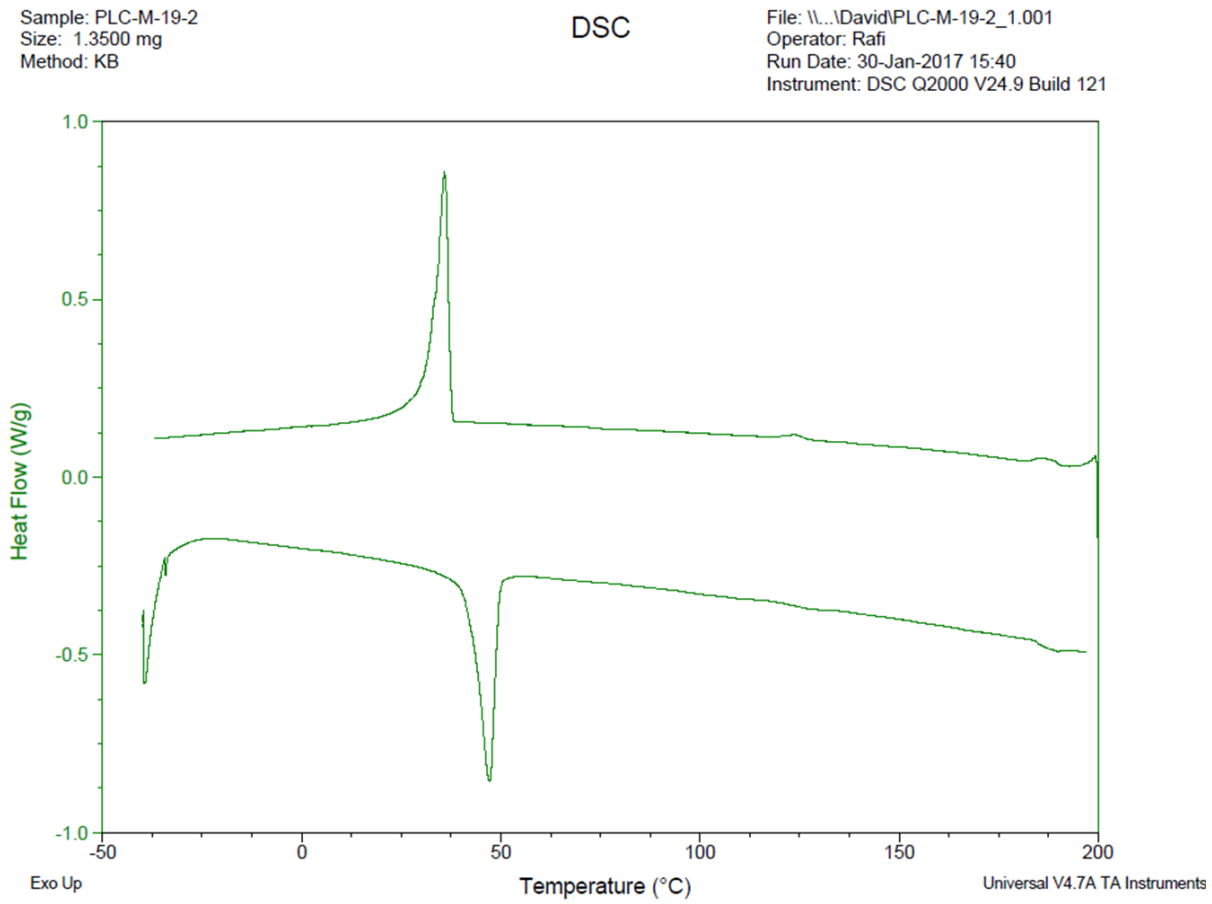

Figure S29. Differential scanning calorimetry thermogram of **β-CD-4** (scan rate 10˚C/min, with one minute isothermal at the end points of the temperature range)**.**

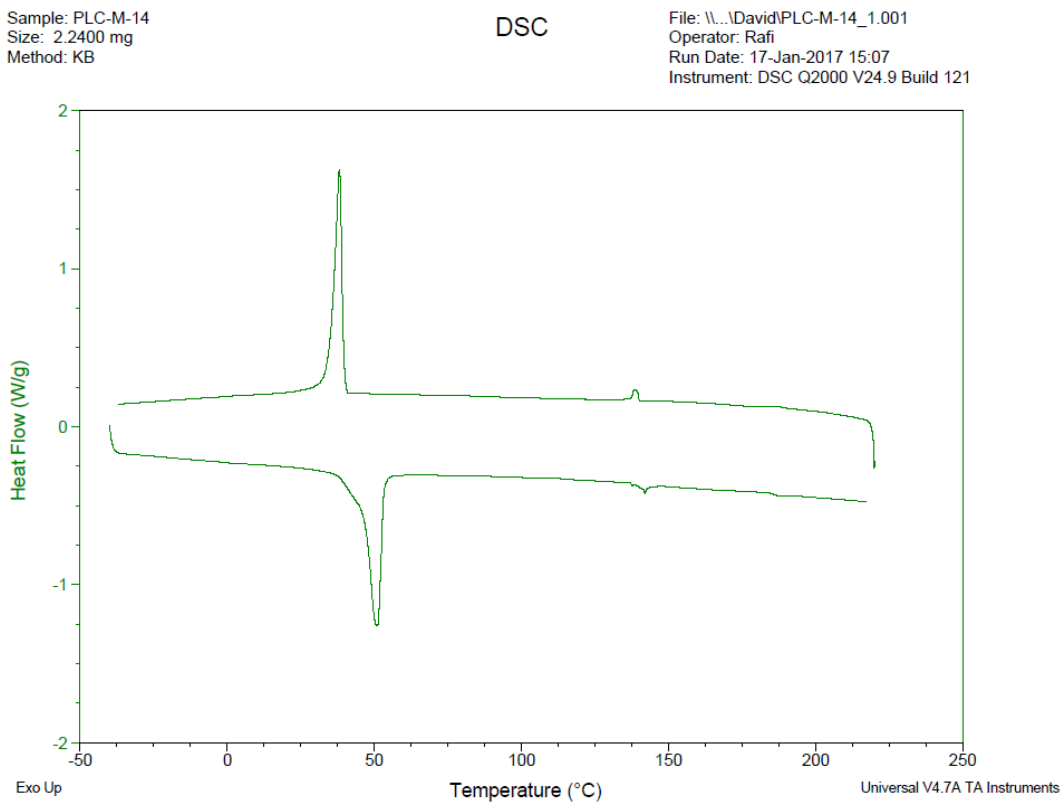

Figure S30. Differential scanning calorimetry thermogram of **β-CD-5** (scan rate 10˚C/min, with one minute isothermal at the end points of the temperature range).

E: Polarized Optical Microscope Pictures

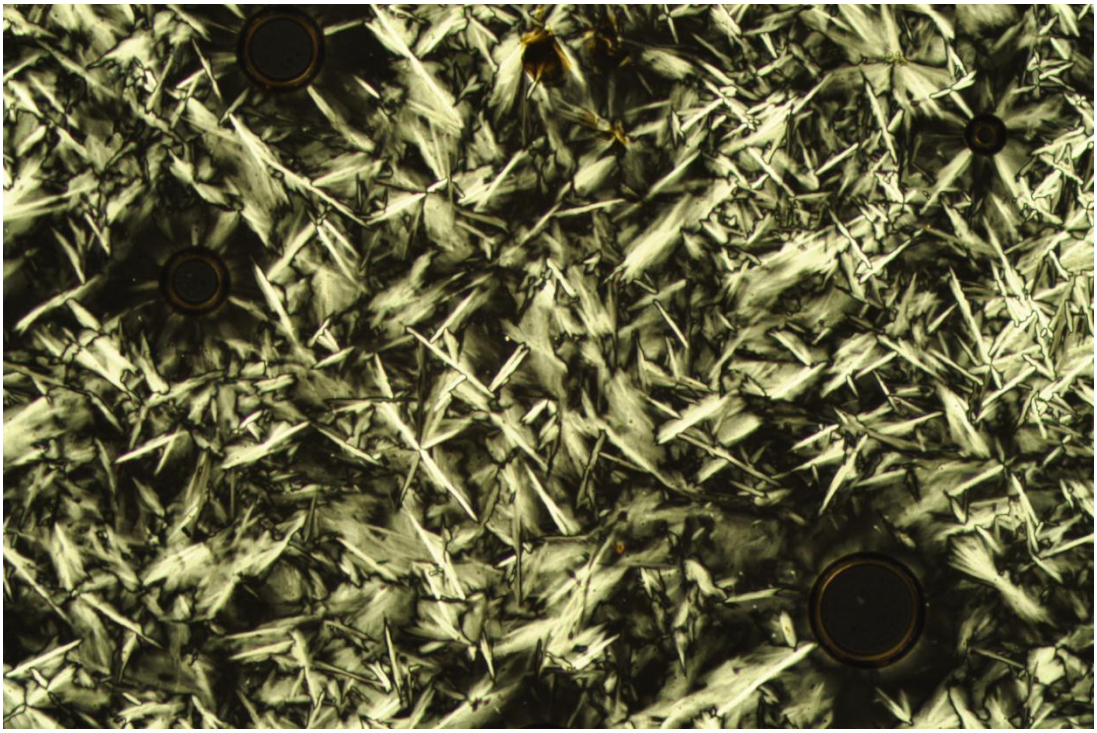

Figure S31. Polarized optical microscope image of **β-CD-4.**

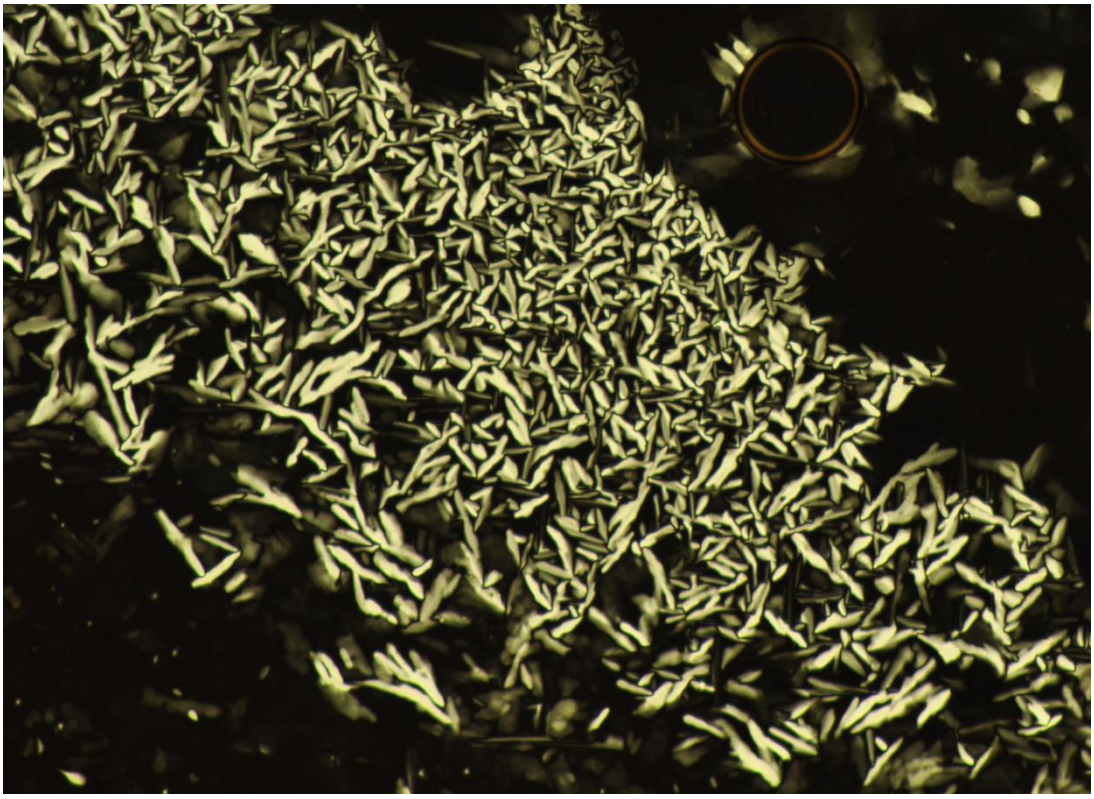

Figure S32. Polarized optical microscope image of **β-CD-4.**

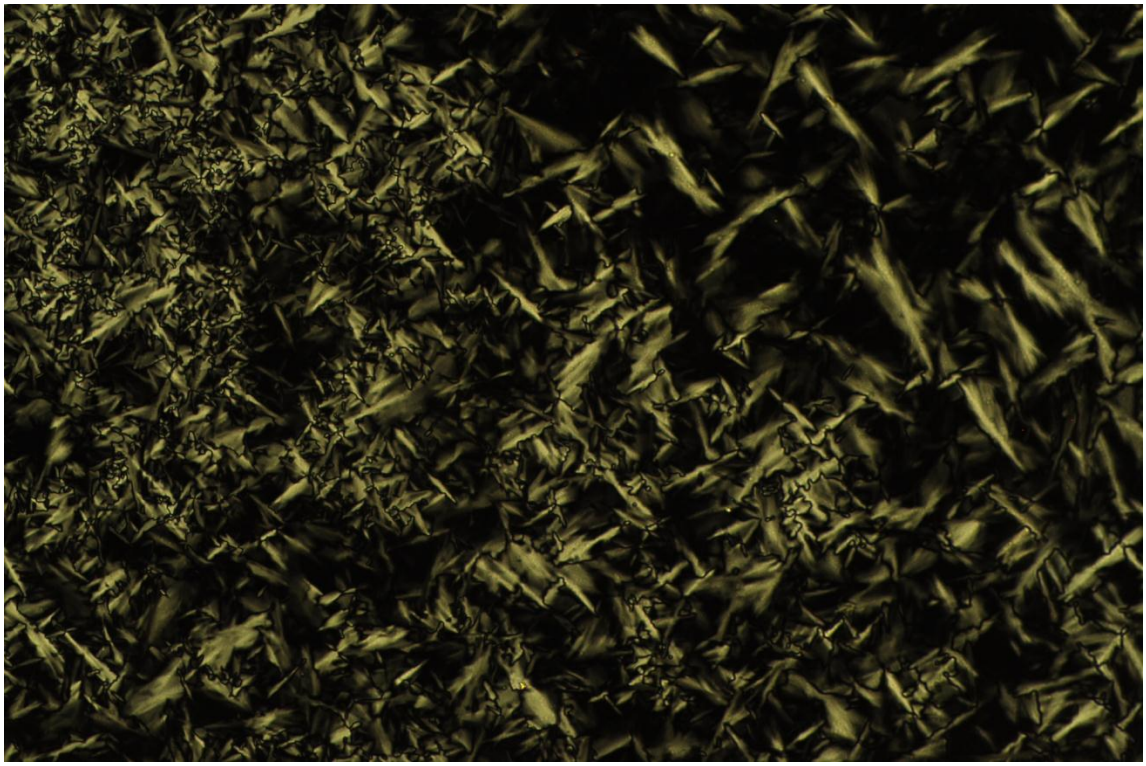

Figure S33. Polarized optical microscope image of **β-CD-5.**

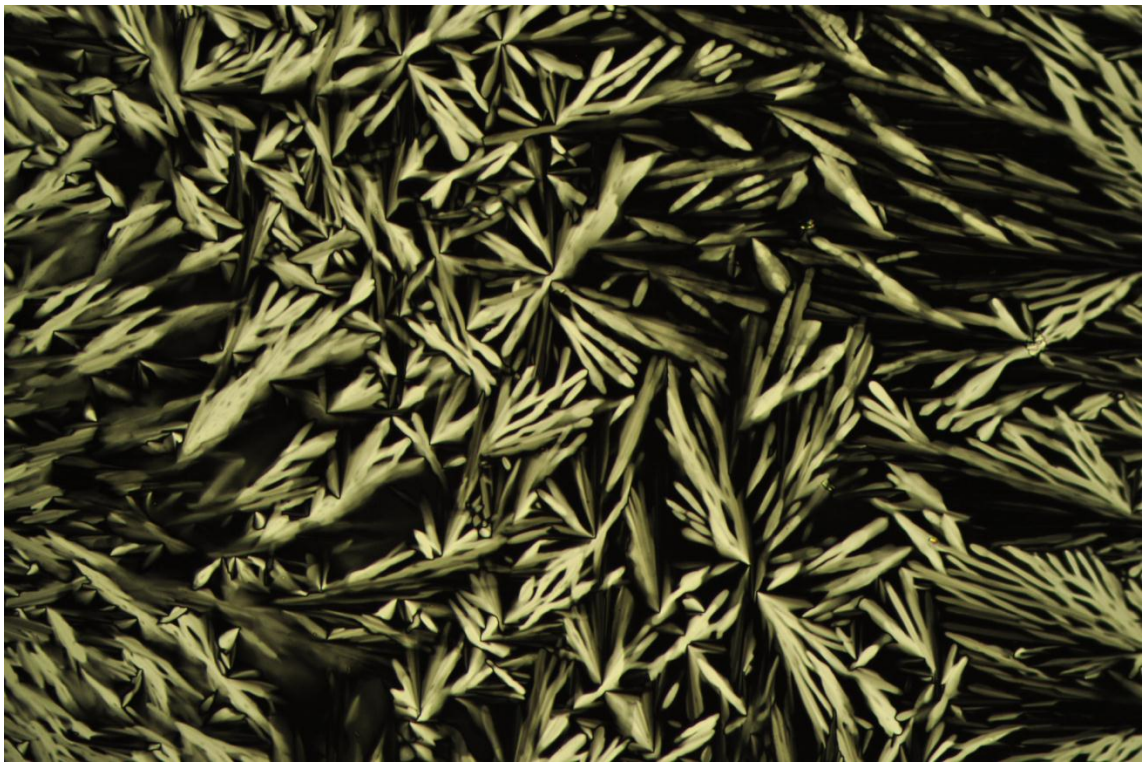

Figure S34. Polarized optical microscope image of **β-CD-5.**

Figure S35. Polarized optical microscope image of **β-CD-5.**

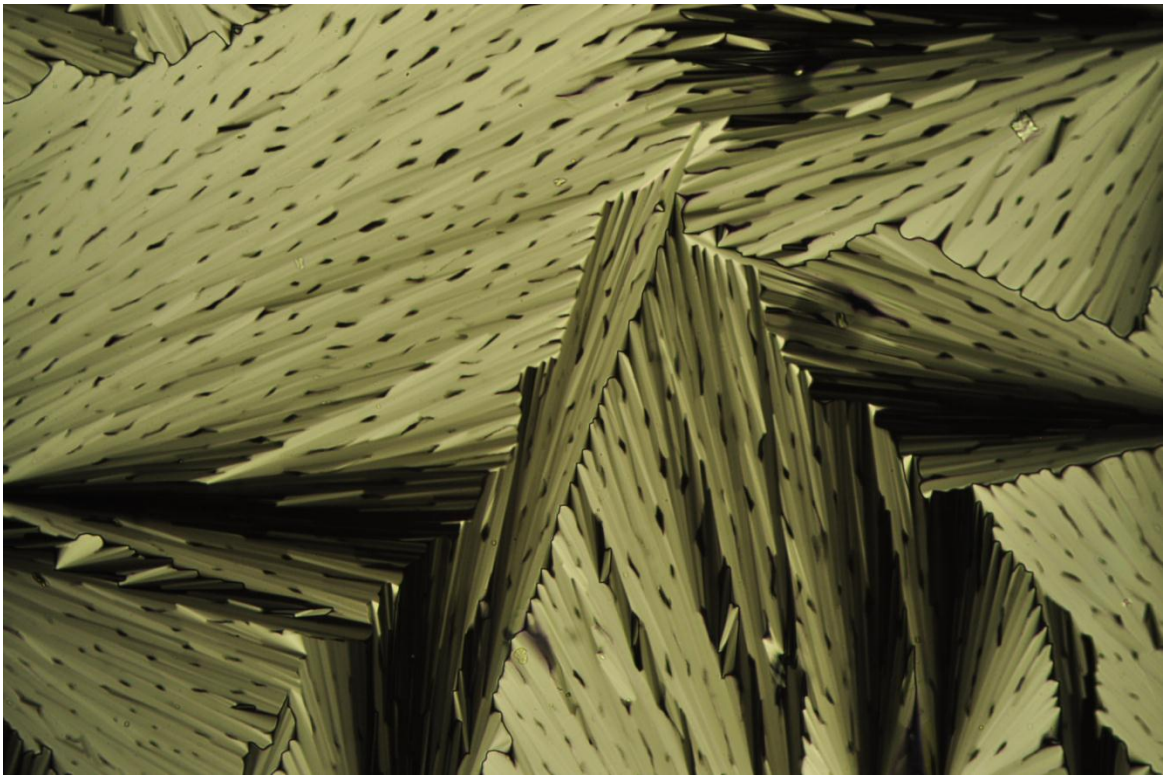

Figure S36. Polarized optical microscope image of **β-CD-5** after clearing point**.**

F: Computational Studies

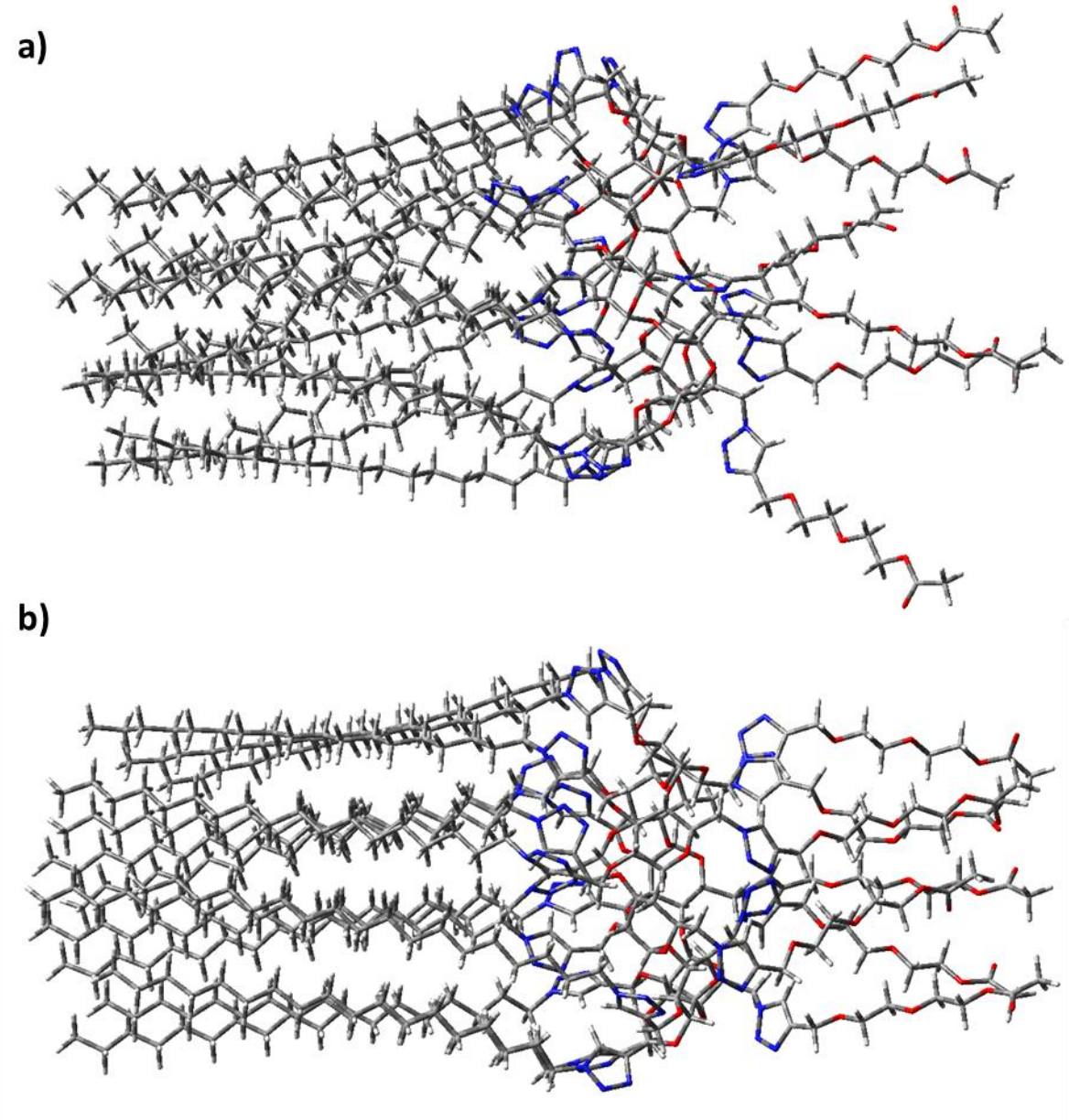

Figure S37. Structure of **β-CD-4** before (a) and after (b) optimization..

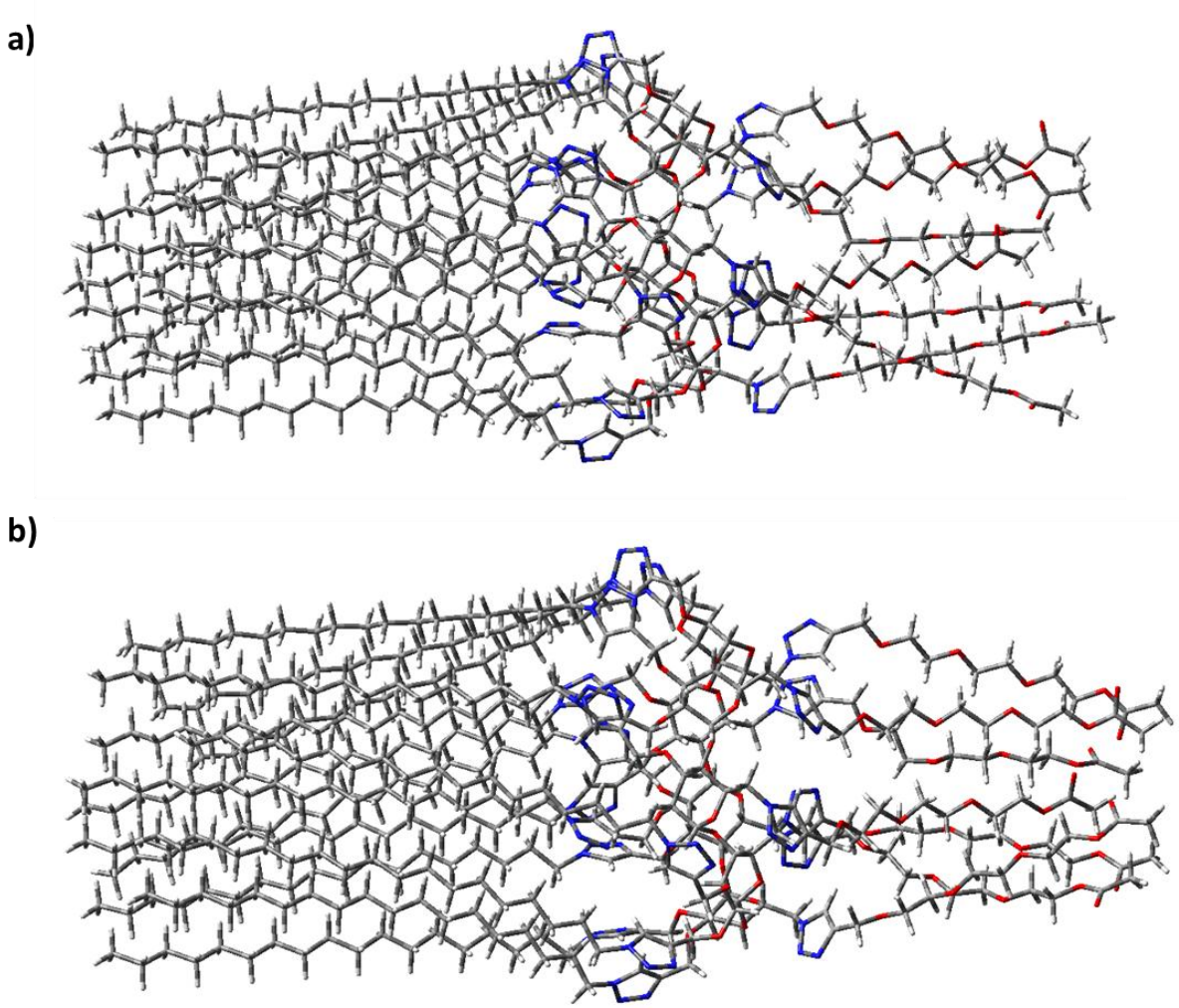

Figure S38. Structure of **β-CD-5** before (a) and after (b) optimization.